NJC

ROYAL SOCIETY OF CHEMISTRY

PAPER

View Article Online
View Journal | View Issue

Cite this: *New J. Chem.*, 2020, **44**, 9264

The structure of the metastable $K_{18}Ta_5Zr_5F_{63}$ phase†

Miroslav Boča, *[a] Maxim Molokeev,[bc] Aydar Rakhmatullin,[d] Blanka Kubíková[a] and Zuzana Netriová[a]

Received 13th May 2020,
Accepted 18th May 2020

DOI: 10.1039/d0nj02428g

rsc.li/njc

A metastable phase $K_{18}Ta_5Zr_5F_{63}$ was prepared by molten salt synthesis of K_2TaF_7 and K_2ZrF_6 in a sealed Pt crucible. This is the first example of a structure of a fluoride complex compound containing both tantalum and zirconium as central atoms. The asymmetric part of the unit cell contains two Ta/Zr sites and one pure Zr site. The Ta1/Zr1 ion is coordinated by seven F ions forming one capped trigonal prism. The Ta2/Zr2 ion is coordinated by six F ions forming a trigonal prism, and this polyhedron is fully ordered. The Zr3 ion is coordinated by six F ions, which are disordered over two positions. All $(Zr/Ta)F_n$ (n = 6–8) polyhedra are isolated from each other, although the ZrF_6 units have shared faces, forming an infinite channel along the c-axis. ^{19}F MAS NMR experiments agree with the proposed structural model, identifying all five central non-equivalent polyhedra. The $K_{18}Ta_5Zr_5F_{63}$ phase decomposes within several months to its initial components; this can be monitored by NMR, DSC and XRD experiments. Moreover, accelerated decomposition can be achieved by thermal treatment, resulting in the formation of a K_3ZrF_7 phase.

Introduction

The chemistry of ternary fluorides is a very broad and complex topic involving hundreds of compounds (all d- and f-elements and some of the p-elements) and numerous investigation methods. Many reviews have been published on the subject, *e.g.*, ref. 1–4. Some of these compounds can be characterized by a strong tendency to form isolated polyhedrons where all fluorine atoms are terminally bonded. Examples include tantalum and niobium fluorides, *e.g.*, ref. 5. We are not aware of any compound of this family containing bridging fluorine atoms. The situation changes when oxygen atoms are also present, *e.g.*, in $K_2Ta_4O_9F_4$ or $K_6Ta_{6.5}O_{14}F_{9.5}$[6,7] compounds, where either oxygen alone or both oxygen and fluorine atoms can serve as bridging elements. However, structures with isolated polyhedra are still dominant. On the other hand, there is a group of compounds with a high tendency to form infinite structural motives in one, two or even three dimensions. This group includes the zirconium fluorides described, *e.g.*, in ref. 8 and references. therein.

The aim of this work is to try to force bridging behaviour on the rigid central atom of tantalum using zirconium as a co-partner, *i.e.*, a central atom with a preference for the bridging mode. The compounds K_2TaF_7 and K_2ZrF_6 were thus selected as suitable candidates. There are many oxide compounds containing both Ta and Zr, such as $Ca_7Zr_7Ta_6O_{36}$,[9] $Ba_6Zr_2Ta_8O_{30}$,[10] and $K_3ZrTa_7O_{21}$.[11] Such crystalline oxide systems with Zr/Ta partial occupations have interesting materials properties.[10] Charge difference for ions at the same lattice site can introduce defects into the structure and modify materials properties. In this paper, we present the first (to the best of our knowledge) example of a fluoride complex compound containing both tantalum and zirconium as central atoms, $K_{18}Ta_5Zr_5F_{63}$.

Results and discussion

Crystal structures of $K_{18}Ta_5Zr_5F_{63}$

The unit cell of $K_{18}Ta_5Zr_5F_{63}$ possesses trigonal/hexagonal symmetry. The space group $P\bar{3}$ was initially assigned on the basis of statistical analysis of the reflection intensities. The crystal structure was solved, but refinement was not good. The Bragg R_B-factor did not decrease any lower than 16%. The twinning of the single crystal with rotation of the unit cell around the [210] direction in real space (Fig. 1S, ESI†) was detected by the PLATON program. Further refinement using the twin matrix

[a] *Institute of Inorganic Chemistry, Slovak Academy of Sciences, Dúbravská cesta 9, SK-845 36 Bratislava, Slovakia. E-mail: miroslav.boca@savba.sk*
[b] *Laboratory of Crystal Physics, Kirensky Institute of Physics, Federal Research Center KSC SB RAS, Akademgorodok 50 bld. 38, Krasnoyarsk, 660036, Russia*
[c] *Siberian Federal University, Krasnoyarsk, 660041, Russia*
[d] *Conditions Extremes et Materiaux, Haute Temperature et Irradiation, 1D avenue de la Recherche Scientifique CS 90055, 45071 Orleans Cedex 2, France*

† Electronic supplementary information (ESI) available: Figures and tables. CCDC 1964932. For ESI and crystallographic data in CIF or other electronic format see DOI: 10.1039/d0nj02428g

Table 1 Crystal structure parameters of $K_{18}Ta_5Zr_5F_{63}$

Total formula	$F_{63}K_{18}Ta_{5.18}Zr_{4.82}$
Dimension (mm)	0.25 × 0.2 × 0.1
Color	Colorless
Molecular weight	3277.80
Temperature (K)	296
Space group, Z	$P6_3/m$, 1
a (Å)	17.3782 (8)
c (Å)	5.8377 (3)
V (Å^3)	1526.80 (16)
ρ_{calc} (g cm^{-3})	3.565
μ (mm^{-1})	11.458
Reflections measured	22 649
Independent reflections	1702
Reflections with $F > 4\sigma(F)$	1647
$2\theta_{max}$ (°)	61.072
h, k, l – limits	$-24 \le h \le 24$; $-24 \le k \le 24$; $-8 \le l \le 8$
R_{int}	0.0583
The weighted refinement of F^2	$w = 1/[\sigma^2(F_o^2) + (0.076P)^2 + 58.01P]$, where $P = (F_o^2 + 2F_c^2)/3$
Number of refinement parameters	60
R_1 [$F_o > 4\sigma(F_o)$]	0.0855
wR_2	0.2241
Goof	1.223
$\Delta\rho_{max}$ (e Å^{-3})	2.423
$\Delta\rho_{min}$ (e Å^{-3})	−2.832
Extinction coefficient	0.0009 (3)
$(\Delta/\sigma)_{max}$	<0.001

rotation (0 1 0; 1 0 0; 0 0 −1) dropped the R_B-factor to 9%. The ratio of twinned blocks was 54 : 46. After that, the structure test for the presence of missing symmetry elements in PLATON found several additional elements, putting the structure in the $P6_3/m$ space group. However, attempts to solve the crystal structure in $P6_3/m$ space group failed due to twinning. In any case, our somewhat roundabout route led to the correct structure and stable refinement (see Experimental part). The main crystal data are shown in Table 1. The atom coordinates and main bond lengths are shown in Tables 1S and 2S (ESI†), respectively.

The asymmetric part of the unit cell contains two Ta/Zr sites: Ta1/Zr1 (6h Wyckoff site with m local symmetry) and Ta2/Zr2 (2c site with $\bar{6}$ symmetry) (Fig. 1), in which the Ta/Zr ratio was refined to 0.69(2) : 0.31(2) and 0.52(2) : 0.48(2), respectively. In addition, there is one pure Zr site (2a site with $\bar{6}$ local symmetry).

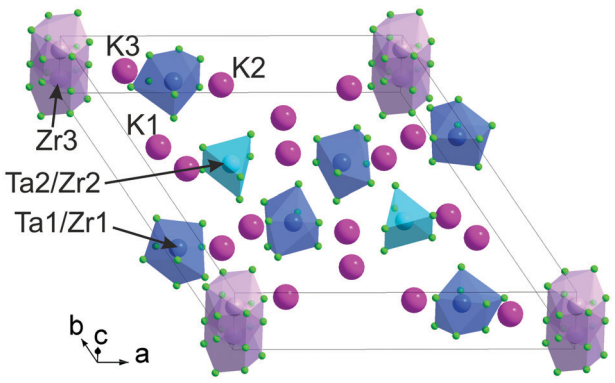

Fig. 1 The crystal structure of $K_{18}Ta_5Zr_5F_{63}$. The heavy ions in the asymmetric unit are labelled.

The Ta : Zr ratio in compound thus appeared to be 5.18 : 4.82. There are three K sites in the structure, all in a 6h Wyckoff site with m local symmetry. There are seven F ions in the asymmetric part of the unit cell, and two sites (F5 and F7) are half-occupied. The total amount of F ions in the unit cell is 63 and the chemical formula can be written as $K_{18}Ta_{5.18}Zr_{4.82}F_{63}$, or simplified to $K_{18}Ta_5Zr_5F_{63}$. The sum of charges is zero − 18 + 5 × (5 + 4) − 63 = 0 – which is additional evidence for the correctness of the structure. The Ta1/Zr1 ion is coordinated by eight F ions, forming a two capped trigonal prism. It should be noted that the F5 ion forms the second cap of this prism, and that this site is only half-occupied. We conjecture that half of the unit cells contain a (Ta1/Zr1)F_7 mono-capped prism, and that the other half contain a (Ta1/Zr1)F_8 two capped prism in the crystal. The XRD experiment averages the structure over space and time, leading to a (Ta1/Zr1)$F_7F_{0.5}$ polyhedron. The Ta2/Zr2 ion is coordinated by six F ions, forming a trigonal prism, and this polyhedron is fully ordered. The Zr3 ion is coordinated by twelve F ions, which from a symmetry point of view are all equivalent, and are thus considered as one (F7) ion multiplied by the various symmetry. Since F7 has occupancy 0.5, in actuality the Zr3 ion is coordinated by six F ions, which are disordered over two positions. All (Zr/Ta)F_n (n = 6–8) polyhedra are isolated from each other, although ZrF_6 adjoin each other facewise, forming an infinite channel along the c-axis (Fig. 1). A similar bridging of zirconium polyhedrons was observed also during phase transformation of pure K_2ZrF_6.[12]

Table 2 provides examples of compounds having either tantalum or zirconium as a central atom, together with Ta/Zr–F distances. As can be seen, the bridging distances (in the case of zirconium) are generally longer than the terminal bonds. Terminal Ta/Zr–F bonds in $K_{18}Ta_5Zr_5F_{63}$ span the range of other fluorido-tantalates/zirconates with coordination number 6, 7 or 8. A more detailed review of the structure of fluorido-tantalates/niobates or/zirconates can be found in ref. 5 and 8.

The values of bond lengths should be considered together with esd values. For example, (Ta1/Zr1–F) = 1.89 Å is actually 1.89(3) Å from our structure. In the International Tables average bond length d(Zr–F) = 2.03(10) Å can be found which was calculated using 66 compounds from CSD (smallest d(Ta–F) = 1.915 Å). The average bond length d(Ta–F) = 1.91(6) Å using 29 compounds from CSD (smallest d(Ta–F = 1.789 Å)). This interval from 2.03(10) Å to 1.91(6) Å intercept with 1.89(3) Å within less than 3esd. Similarly, the average d(K–F) = 2.7(2) Å (smallest 2.418 Å) among 354 compounds (IT tables). In our case d(K3–F7) = 2.38(5) Å what spans to the interval within 2esd. Relatively short F–F contact appears only due to presence of disordering, which is common situation. It must be noted that abnormally short Zr–F distances were also observed for some K_2ZrF_6 polymorphs[12] similarly as was done in this work. Due to the above described complications (and also those described in NMR part and experimental part below) the proposed structure should be considered as structural model rather than the perfectly solved structure. Some other aspects like merohedral or pseudomerohedral twinning cannot be excluded.

It should be noted that if the compound were limited to equimolar amounts of both starting compounds, the resulting

Table 2 Comparison of bond distances in $K_{18}Ta_5Zr_5F_{63}$ and other fluorido-tantalates or zirconates

Polyhedron	Ta/Zr–F distance	System	Ta/Zr–F distance
$(Ta1/Zr1)F_6$	1.89–2.18 Å	$KTaF_6$[13]	2.15 Å terminal
One capped prism	Terminal	Li_2ZrF_6[14]	2.016 Å terminal
$(Ta1/Zr1)F_7$	1.89–2.18 Å	K_2TaF_7[15]	1.919–1.976 Å terminal
Two caped prism	Terminal	$(NH_4)_3ZrF_7$[16]	1.9733 Å, 2.033 Å terminal
		Na_3ZrF_7[17]	2.291 Å terminal
$(Ta2/Zr2)F_6$	1.87 Å	$KTaF_6$[13]	2.15 Å terminal
Trigonal prism	Terminal	Li_2ZrF_6[14]	2.016 Å terminal
$Zr3F_6$ chains	1.89 Å terminal	K_2ZrF_6[18]	2.0411 Å, 2.081 Å terminal
	2.30 Å bridging		2.1447 Å, 2.206 Å bridging

formula would be K_4TaZrF_{13} or $K_{20}Ta_5Zr_5F_{65}$. This means that during the experiment a more stable system was formed, but one poorer by two KF "molecules" – $K_{18}Ta_5Zr_5F_{63}$ – representing a 3 wt% difference. This situation can be compared to that of the system NaF–ZrF_4, in which equimolar amounts of NaF and ZrF_4 do not give rise to $NaZrF_5$ but rather to the more stable $Na_7Zr_6F_{31}$ phase.[19]

XPS spectroscopy

XPS seems to be the most appropriate method to obtain at least some of needed information. By XPS the presence of elements F, K, Zr (position of 3d signal at 184.5 ppm corresponds to Zr(4+) oxidation state) and Ta (position of 4d signal at 233.0 ppm corresponds to Ta(5+) oxidation state) was proved. However, for analytical purposes some limitations must be considered. The experimental ratio of heavy elements (Ta/Zr) seems to be acceptable giving the value 1.07 (exp.) while the ratio of heavy and light elements cannot be considered correctly (thus these data are omitted). Even the exact chemical composition of the title compound cannot be confirmed (because of the big difference between light and heavy elements), the analysis of a separate signals can be done; confirming the presence of both terminal (dominant) and bridging forms of fluorine atoms, in agreement with the structural investigation and with previous work on methods sensitive to various bonding modes of fluorine atom.[19]

NMR spectroscopy

The room-temperature polymorph contains seven fluorine sites. ^{19}F MAS NMR spectra found two groups of resonances. Applying a very fast spinning frequency (60 kHz) and high field (20.0 T) enabled us to reduce the spectrum to only five signals with a Gaussian line shape. By considering the Ta and Zr atoms' surroundings, it can be seen that the five Ta and Zr atomic positions have few, or only one, distinct fluorine atoms in their coordination spheres: Ta1(2F1, 2F2, 2F3, F4, 0.5F5), Zr1(2F1, 2F2, 2F3, F4, 0.5F5), $Ta2(F6)_6$, $Zr2(F6)_6$, $Zr3(0.5F7)_{12}$. Assuming fast hopping of the fluorine between the positions in its polyhedron, the ^{19}F δ_{iso} is then the average of the individual δ_{iso} values for those positions. The five peaks were thus assigned to fluorine atoms in the five polyhedra (Table 3 and Fig. 2). The low-field signals have chemical shift values close to K_2TaF_7 (17.1 ppm) and K_3TaF_8 (17.3 ppm) compounds,[5] and we attribute them to fluorine atoms connected with Ta atoms. The high-field peaks can be assigned to fluorine atoms connected with Zr atoms.[8] It is worth mentioning that the same dynamic behaviour of fluorine atoms was observed in the case of K_2TaF_7.[5] The intensity ratio of the two environments I[Ta]/I[Zr] = 0.53/0.47 is in rather good agreement with the value of 0.518/0.482 expected from the sites' multiplicities and occupations. There are differences between the expected and observed integral data for the tantalum polyhedra. A possible reason for this ambiguity is signal overlay. The reasonably good agreement between the expected and experimental integral intensities enables us to perform spectral assignment of the NMR resonances to the crystallographic sites. Small amounts of a secondary unknown phase were observed at 13.4 ppm. It seems to be a typical problem in ternary fluorides of Ta and Zr that number of crystallographically equivalent fluorines often does not correspond to the number of obtained NMR signal due to several reasons. The experimental data were presented and discussed for both pure compounds K_2TaF_7 and K_2ZrF_6 in previous works.[5,8]

Table 3 Experimental ^{19}F MAS NMR isotropic chemical shifts δ_{iso}, integral intensities, and simulated integral intensities

	δ_{iso}, ppm (±0.1 ppm)	Integral intensity, % (±1%)	Simulated integral intensity, %
Ta2	15.9	19	10.4
Ta1	15.1	34	41.4
Zr1	−16.7	17	18.6
Zr3	−17.6	18	20.0
Zr2	−18.8	12	9.6

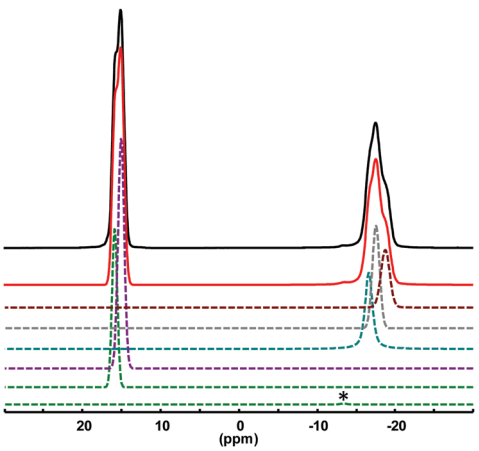

Fig. 2 ^{19}F MAS NMR experimental (black line) spectrum and its simulation (red line). Decomposition of the theoretical spectrum in its individual components (coloured dashed curves), (* secondary phase).

The appearance of metastable phases was documented also in relatively simple systems of binary MgF_2–MF_2 (M = Ca, Sr). (Ca or Sr)MgF_4 can only be observed in a mixture accompanied by the binary fluorides. They are metastable and disappear after thermal annealing.[20]

It must be noted that the sample underwent thermal decomposition as well as decomposition over time. ^{19}F MAS NMR and XRD of the sample measured three months after synthesis showed almost complete decomposition into the initial phases K_2TaF_7 and K_2ZrF_6 (Fig. 2S, ESI†). This process supports the idea implied by the NMR data of fast hopping of the fluorine ions between various positions, resulting in the stabilisation of the system.

DSC measurements

DSC measurements on a fresh sample showed the presence of one weak endothermic effect at 801 K (0.1505 J g^{-1} equal to 493.3 J mol^{-1}) within the heating regime of up to 827 K. (This target temperature was selected from consideration of the phase diagram of K_2TaF_7–K_2ZrF_6, being far below the liquid phase of the $x(K_2TaF_7)$ = 0.5 point.[21]) However, during the cooling regime, no identifiable effect was observed. XRD of the sample used in the DSC experiment showed the presence of $K_{18}Ta_5Zr_5F_{63}$, together with a small amount of K_3ZrF_7.

DSC treatment of a one-month-old sample heated up to 1173 K showed three endothermic effects at 940 K, 961 K and 988 K (this last one can be attributed to melting). The existence of three such effects has been documented for the pure K_2TaF_7 phase (although with somewhat higher temperatures).[22–24] XRD of the solidified sample showed the presence of $K_{18}Ta_5Zr_5F_{63}$, but with K_3ZrF_7 present as the dominant phase.

DSC treatment of a two-month-old sample found two endothermic signals at 507 K and 555 K that are quite similar to those of pure K_2ZrF_6.[25] At *ca.* 1023 K the sample starts to evaporate, with a mass loss of *ca.* 25 wt% up to 1173 K. Three other, poorly-resolved and overlapping, endothermic effects were observed at 884 K, 935 K, and 958 K, also typical for the K_2TaF_7 phase but at even lower temperatures than in the case of the one-month-old sample (Fig. 3S, ESI†).

The X-ray powder pattern transformation under sample heating is presented in Fig. 3. One can see that additional peaks appear at 543 K (Fig. 3b). Their intensities increase under further heating. The peaks of the main phase, $K_{18}Ta_5Zr_5F_{63}$, totally disappear at 663 K, and the remaining peaks are associated with the cubic phase $Fm\bar{3}m$ isostructural to K_3ZrF_7. The thermal dependencies of the main phase cell parameters *a* and *c* (Fig. 4), show a linear trend only in the range of 303–543 K. This indicates that the $K_{18}Ta_5Zr_5F_{63}$ phase is only stable up to 543 K, and that further heating decomposes it to form a cubic phase which is isostructural to K_3ZrF_7.

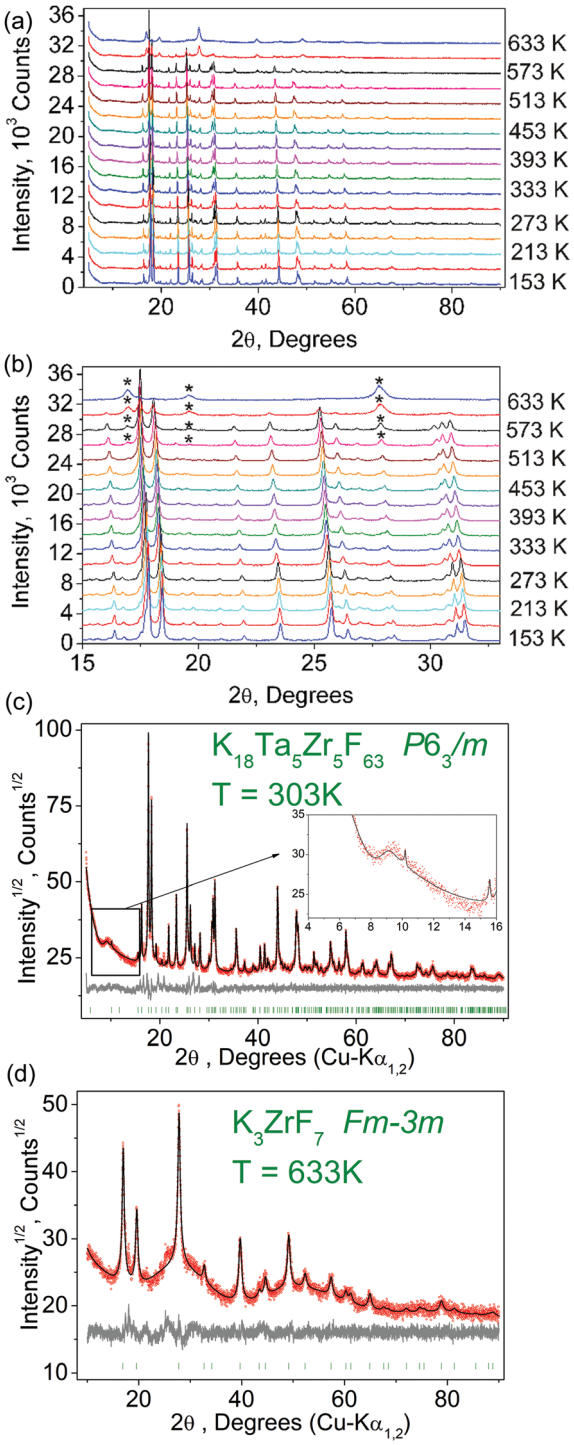

Fig. 3 The X-ray pattern transformation of $K_{18}Ta_5Zr_5F_{63}$ under heating from 153 K to 633 K (a-top). Zooming in on part of these patterns (b) reveals the appearance of impurity peaks (marked by stars) at 543 K, which may be associated with the K_3ZrF_7 isostructural phase. The main peak intensities of $K_{18}Ta_5Zr_5F_{63}$ decrease between 543 and 633 K and totally disappear at 633 K. $K_{18}Ta_5Zr_5F_{63}$ thus transforms to a cubic phase isostructural to K_3ZrF_7. Difference powder pattern plots of $K_{18}Ta_5Zr_5F_{63}$ at 303 K (c) and K_3ZrF_7 at 633 K (d-bottom) show that these two end phases are almost pure.

Experimental

Preparation of sample

For the preparation of the sample, the following chemicals were used:

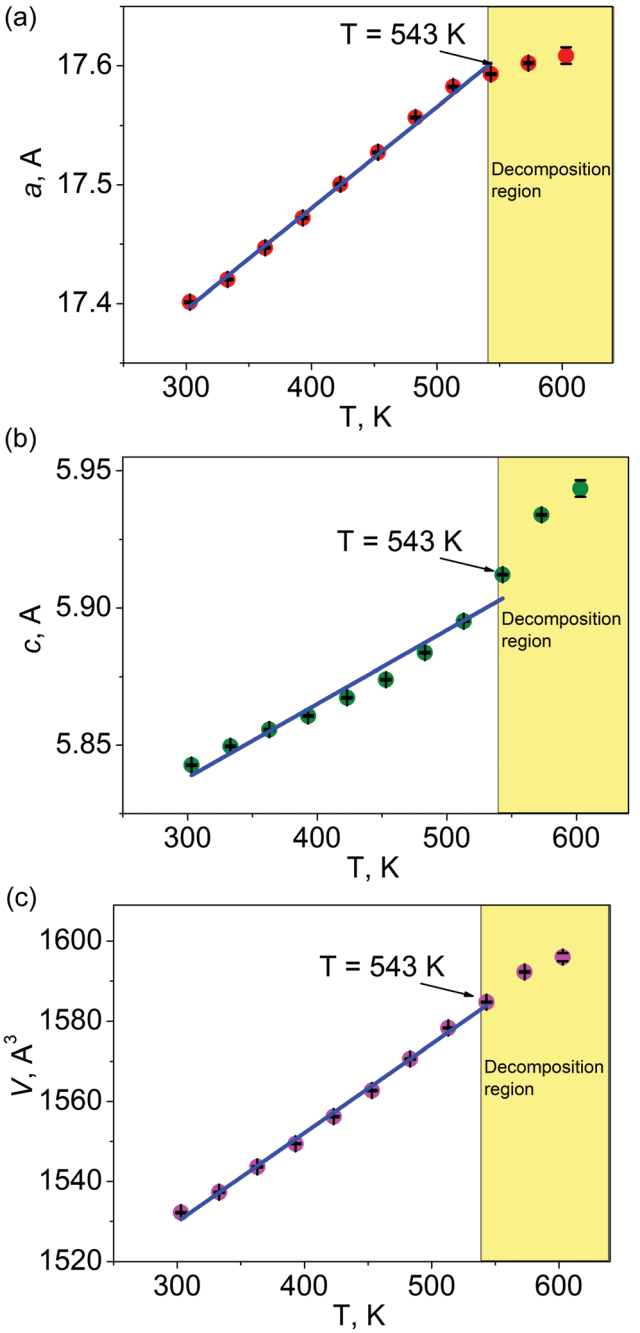

Fig. 4 Thermal dependencies of cell parameters (as rate of change per unit temperature): (a) *a* cell parameter; (b) *c* cell parameter; (c) cell volume *V*(T).

K_2TaF_7 was prepared at the Institute of Chemistry and Technology of Rare Elements and Minerals, RAS Apatite-Russia, 99.5%. K_2ZrF_6 was prepared as described in ref. 25.

A finely-powdered and homogenized mixture of K_2TaF_7 (0.830 g, 2.15 mmol) and K_2ZrF_6 (0.609 g, 2.15 mmol) was placed in a platinum crucible with a sealed lid. The narrow platinum tube on the top of the lid, which served for loading of the sample into the crucible, was closed first by clamping and then by welding. Homogenizing and weighing the sample was done in a glove box under a dry inert atmosphere. The crucible was placed in a furnace and heated to 1153 K at a rate of 5 K min^{-1} and then heated to 1173 K at a rate of 1 K min^{-1}. The temperature of the furnace was kept at 1173 K for 120 min and cooled at a rate of 1 K min^{-1} to room temperature. The platinum crucible was opened and the sample was separated as a white cake. Several single crystals were separated by sieving and the rest was powdered for investigation by various diffraction and spectroscopic methods.

Structural analysis

XRD intensity patterns were collected for single crystals of $K_{18}Ta_5Zr_5F_{63}$ at 296 K using the SMART APEX II X-ray single crystal diffractometer (Bruker AXS, analytical equipment of the Krasnoyarsk Center for the collective use of SB RAS) equipped with a CCD-detector Photon2, graphite monochromator and Mo Kα radiation source. Absorption corrections were applied using the SADABS program. The structures were solved by direct methods using the package SHELXS; structural refinement, using the anisotropic approach for heavy atoms and the isotropic approach for F ions, was performed with the SHELXL program.[26] The structure test for the presence of missing symmetry elements and possible voids was carried out using the program PLATON.[27] The DIAMOND program was used for crystal structure plotting.[28]

An *ab initio* structure solution using $P6_3/m$ failed. But it was successfully solved in $P\bar{3}$. After clarification the situation with twinning, the model $P\bar{3}$ was greatly improved. The consequent crystal structure checking in PLATON revealed several additional symmetry elements which were missed. Thus the $P\bar{3}$ model was changed to $P6_3/m$ and after that $P6_3/m$ was successfully refined using twinning. Refinement in $P6_3/m$ was stable and gave good *R*-factors. Crystal structure was checked using CheckCIF tool and there were no unexplained Alerts, thus the structure was considered to be correct. PLATON software didn't detect any problems with voids, symmetry also. One Alert that F1···F5 contact is short (1.96 Å) can be associated with the fact that F5 ion is disordered (has 0.5 occupancy). Usually the coordinates of disordered ions cannot be refined very well. Some thermal parameters of ions have relatively high values due to presence of disordering also. Twinning effect also could have influence on it.

Powder X-ray diffraction

XRD data of $K_{18}Ta_5Zr_5F_{63}$ were obtained using a D8 ADVANCE diffractometer in Bragg–Brentano geometry (Bruker, analytical equipment of the Krasnoyarsk Center for the collective use of SB RAS) equipped with a VANTEC detector with a Ni filter and Cu Kα radiation source. An Anton Paar TTK450 attachment was used for all temperature measurements over the range of 153–633 K (Fig. 3a and b). Each pattern was measured over a 2θ range of 5–90° with a 0.6 mm divergence slit; the step size of 2θ was 0.016°, and the counting time was 0.4 s per step. Le Bail profile fitting[29] was carried out using the program TOPAS 4.2.[30] The low *R*-factors and good refinement results shown in Table 3S (ESI†), indicate the crystal structures of the powder samples to be representative of the $K_{18}Ta_5Zr_5F_{63}$ bulk structure. Powder pattern was fitted very well using cell parameters obtained from single crystal experiment. As for 2θ 4–15 region,

there are three calculated peaks. First one peak is hidden in $1/x$ high background, it impossible to see small peaks in this region. Second peak is clearly seen on zoomed figure Fig. 3c. Third peak probably has very low intensity and current pattern has too big noise to reveal it. Anyway, all other peaks were fitted very well and unit cell was obtained from single crystal experiment.

DSC analysis

The thermal properties of the studied compounds were investigated by means of DSC methods performed with a NETZSCH Simultaneous Thermal Analyzer STA 449 F1 Jupiter®. The sample ($m_0 \approx 20.45$ mg) was placed in a Pt/Rh (80/20) crucible and enclosed in an STA apparatus. The system was evacuated three times, and then measured under an argon atmosphere (244 mL min^{-1}). The experimental thermogram was recorded over a temperature regime ranging from 293 K to 1173 K and back with a heating/cooling rate of 5 K min^{-1}. A baseline correction measurement for the empty crucible was done under the same conditions as the sample measurements. Calibration of temperature (for Pt crucibles) and sensitivity (±3%) was done for the compounds $C_{12}H_{10}$, $RbNO_3$, Ag_2SO_4, CsCl, K_2CrO_4 and $BaCO_3$. The NETZSCH Proteus Thermal Analysis software was used for data processing and for evaluation of the experimental thermogram.

X-ray photoelectron spectroscopy

XPS signals were recorded using a Thermo Scientific K-Alpha XPS system (Thermo Fisher Scientific, UK) equipped with a micro-focused, monochromatic Al Kα X-ray source (1486.6 eV). An X-ray beam of 100 μm size was used at 1.16 mA × 12 kV. The spectra were acquired in the constant analyzer energy mode with a pass energy of 50 eV for the whole region, which ranged from 10 eV to 1100 eV with an energy step size of 0.1 eV. Charge compensation was achieved using a flood gun incorporated into the system, providing both low energy electrons (~0 eV) and low energy argon ions (20 eV) from a single source. The argon partial pressure was 2×10^{-7} mbar in the analysis chamber. The position of the C1s signal of adventitious carbon was 284.7 eV for all samples, so it was not necessary to do charge correction using this internal reference. The Thermo Scientific Avantage software, version 5.948 (Thermo Fisher Scientific), was used for digital acquisition and data processing. Spectral calibration was carried out by using the automated calibration routine and the internal Au, Ag and Cu standards supplied with the K-Alpha system. The Powel fitting algorithm was used with 100 iterations to fit the XPS F1s peaks. The line shapes were products of a Lorentz/Gauss mixture, with the ratio fixed at L/G = 45%. This value was taken from fitting the F1s peak of pure NaF, with this parameter permitted to vary using the Powel algorithm. The analysis was done on a sample at a fresh crack in order to eliminate surface impurities.

NMR spectroscopy

Room-temperature ^{19}F NMR spectra were recorded on a Bruker AVANCE Neo 850 NMR spectrometer with a 20 T magnet operating at 800.0 MHz for ^{19}F nuclei. A standard Bruker MAS probehead was used with a 1.3 mm rotor, wherein powder was rotated at 60 kHz. The pulse width was 0.71 μs, and the pulse delay was 2.6 s ($5 \times T_1$). The ^{19}F chemical shift was referenced to $CFCl_3$. The real temperature of the sample, according to our measurements at "room temperature" and using 60 kHz MAS, is 338 K (65 °C).[8]

Conclusions

For the first time, a fluoride containing Ta and Zr as mixed central atoms has been presented. The metastable phase $K_{18}Ta_5Zr_5F_{63}$ was prepared by molten salt synthesis from K_2TaF_7 and K_2ZrF_6. Its structure was determined from single crystal structural analysis, and the suggested model was confirmed by ^{19}F MAS NMR experiments. Fast averaging of F ions over positions within a polyhedron was detected for all polyhedra using solid state NMR. The decomposition over time of the metastable phase was observed: under isothermal conditions at ambient temperature the phase decomposed to its initial phases, while during thermal treatment and decomposition the K_3ZrF_7 phase was formed as one of the products.

Conflicts of interest

There are no conflicts to declare.

Acknowledgements

Financial support from TGIR-RMN-THC Fr3050 CNRS for conducting the research is gratefully acknowledged. This work was supported by the Slovak Research and Development Agency under the contract no. APVV-15-0479. This work was financially supported by the Scientific Grant Agency of the Ministry of Education of the Slovak Republic and the Slovak Academy of Sciences, grant no. Vega 2/0024/20.

Notes and references

1 M. Leblanc, V. Maisonneuve and A. Tressaud, *Chem. Rev.*, 2015, **115**, 1191–1254.
2 P. P. Fedorov, A. A. Luginina, S. V. Kuznetsov and V. V. Osiko, *J. Fluorine Chem.*, 2011, **132**, 1012–1039.
3 B. P. Sobolev and P. P. Fedorov, *J. Less-Common Met.*, 1978, **60**, 33–46.
4 P. P. Fedorov, *Russ. J. Inorg. Chem.*, 1999, **44**, 1703–1727.
5 M. Boca, A. Rakhmatullin, J. Mlynarikova, E. Hadzimova, Z. Vaskova and M. Micusik, *Dalton Trans.*, 2015, **44**, 17106–17117.
6 J. P. Chaminade, M. Vlasse, M. Pouchard and P. Hagenmul, *Bull. Soc. Chim. Fr.*, 1974, 1791–1794.
7 M. Vlasse, A. Boukhari, J. P. Chaminade and M. Pouchard, *Mater. Res. Bull.*, 1979, **14**, 101–108.
8 A. Rakhmatullin, M. Boča, J. Mlynáriková, E. Hadzimová, Z. Vasková, I. B. Polovov and M. Mičušík, *J. Fluorine Chem.*, 2018, **208**, 24–35.

9 S. Schmid, J. G. Thompson, R. L. Withers, C. D. Ling, N. Ishizawa and S. Kishimoto, *Acta Crystallogr., Sect. B: Struct. Sci.*, 1999, **55**, 313–320.
10 E. O. Chi, A. Gandini, K. M. Ok, L. Zhang and P. S. Halasyamani, *Chem. Mater.*, 2004, **16**, 3616–3622.
11 I. V. Odynets, A. A. Babaryk, V. N. Baumer, N. S. Slobodyanik and O. V. Shiskin, *Z. Anorg. Allg. Chem.*, 2011, **637**, 1511–1515.
12 L. Smrcok, A. Le Bail, M. Boca and A. Rakhmatullin, *Cryst. Growth Des.*, 2020, DOI: 10.1021/acs.cgd.0c00166.
13 H. Bode and H. Vondohren, *Acta Crystallogr.*, 1958, **11**, 80–82.
14 G. Brunton, *Acta Crystallogr., Sect. B: Struct. Sci.*, 1973, **29**, 2294–2296.
15 C. C. Torardi, L. H. Brixner and G. Blasse, *J. Solid State Chem.*, 1987, **67**, 21–25.
16 A. A. Udovenko and N. M. Laptash, *J. Struct. Chem.*, 2008, **49**, 482–488.
17 L. Harris, *Acta Crystallogr.*, 1959, **12**, 172.
18 A. V. Gerasimenko, I. A. Tkachenko, V. Y. Kavun, N. A. Didenko and V. I. Sergienko, *Russ. J. Inorg. Chem.*, 2006, **51**, 9–22.
19 M. Boča, P. Barborík, M. Mičušík and M. Omastová, *Solid State Sci.*, 2012, **14**, 828–832.
20 G. Scholz, S. Breitfeld, T. Krahl, A. Düvel, P. Heitjans and E. Kemnitz, *Solid State Sci.*, 2015, **50**, 32–41.
21 B. Kubíková, J. Mlynáriková, Z. Vasková, P. Jeřábková and M. Boča, *Monatsh. Chem.*, 2014, **145**, 1247–1252.
22 L. Kosa, I. Mackova, I. Proks, O. Pritula, L. Smrcok, M. Boca and H. Rundlof, *Cent. Eur. J. Chem.*, 2008, **6**, 27–32.
23 B. Kubikova, M. Boca and M. Gaune-Escard, *Monatsh. Chem.*, 2008, **139**, 587–590.
24 M. Boca, V. Danielik, Z. Ivanova, E. Miksikova and B. Kubikova, *J. Therm. Anal. Calorim.*, 2007, **90**, 159–165.
25 M. Boča, Z. Netriová, A. Rakhmatullin, Z. Vasková, E. Hadzimová, Ľ. Smrčok, O. Hanzel and B. Kubíková, *J. Mol. Liq.*, 2019, 110969.
26 G. M. Sheldrick, *Acta Crystallogr., Sect. A: Found. Crystallogr.*, 2008, **64**, 112–122.
27 *PLATON, A Multipurpose Crystallographic Tool*, Utrecht University, Utrecht, The Netherlands, 2008.
28 K. Brandenburg and M. Berndt, DIAMOND – Visual Crystal Structure Information System CRYSTAL IMPACT, Postfach 1251, D-53002 Bonn.
29 A. Le Bail, H. Duroy and J. L. Fourquet, *Mater. Res. Bull.*, 1988, **23**, 447–452.
30 *Bruker AXS TOPAS V4: General profile and structure analysis software for powder diffraction data – User's Manual*, Bruker AXS, Karlsruhe, Germany, 2008.

